Journal of Materials Chemistry

Dynamic Article Links ►

Cite this: DOI: 10.1039/c0xx00000x

www.rsc.org/xxxxxx

Paper

Electronic Supplementary Information

Low Temperature Synthesis and SERS Application of Silver Molybdenum Oxides

Essy Kouadio Fodjo,[a] Da-Wei Li,*[a] Niamien Paulin Marius,[b] Trokourey Albert[b] and Yi-Tao Long,*[a]

Received (in XXX, XXX) Xth XXXXXXXXX 20XX, Accepted Xth XXXXXXXXX 20XX
DOI: 10.1039/b000000x

S1. Characterization of silver molybdenum oxides

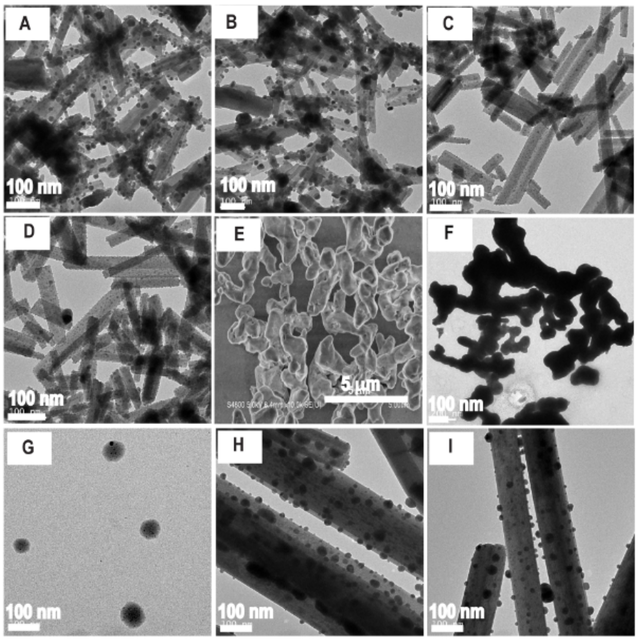

Fig. S1. TEM images of silver molybdenum oxide synthesized at pH (A) 1, (B) 2, (C) 3, (D) 5, (F) 8 and (G) 12 using glucose, (H) 1 using cysteamine, (I) 1 by converting $Ag_2Mo_2O_7$ using cysteamine, and (E) SEM image of silver molybdenum oxide synthesized at pH 8.

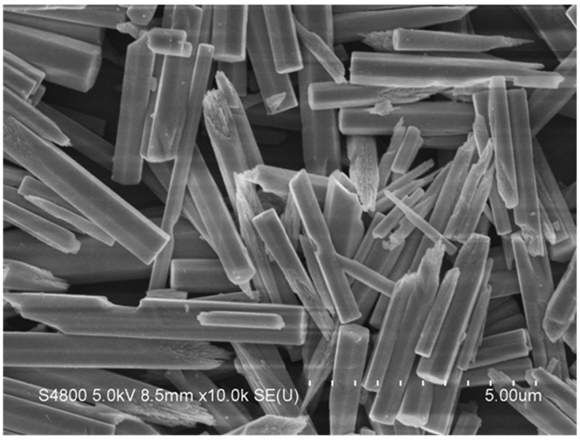

Fig. S2. SEM image of silver molybdenum oxide synthesized at pH 2 using glucose

The synthesized products as indicated in **Fig. S1**, are constituted of nanowires covered by Ag nanoparticles in acidic media while in basic media, the nanomaterials are essentially nanospheres or nanospheres aggregation. It should be noted that the nanowires obtained at pH = 2, are hexagonal (**Fig. S2**). The crystalline parameters of as-synthesized product at different pH are assigned in **Table S1**. As displayed in **Table S1**, the size the nanoparticles of which constituted nanomaterials decrease whith the increase of the pH, and different morphology and crystalline types are obtained.

Table S1. Crystalline parameters of synthesized silver molybdenum oxides.[S1,S2,S3]

pH	Lattice parameters			Interaxial angle			Nature of crystal	Structure of nanomaterial	Size of	
	a/Å	b/Å	c/Å	α/°	β/°	γ/°			Nanowires/nm	Ag NPs/nm
12		4.078 ±0.003			90		Cubic Ag/Mo*	Nanospheres	~70	
8		9.312 ±0.002			90		Cubic Ag_2MoO_4	Nanosphere aggregations	65-80	
5	6.127 ±0.042	13.079 ± 0.102	7.978 ±0.065	90	114.5±5.2	90	Monoclinic $Ag_2Mo_2O_7$	Nanowires covered by Ag NPs	70-300	6-13
3	7.397 ±0.248	5.445 ±0.044	5.742 ±0.099	90	92.4±5.3	90	Monoclinic Ag/β-MoO_3	Nanowires covered by Ag NPs	70-400	6-16
2	10.588 ± 0.019		14.972 ± 0.061		90	120	Hexagonal Ag/h-MoO_3	Nanowires covered by Ag NPs	100-500	10-29
1	3.858 ±0.125	13.886 ± 0.042	3.739 ± 0.031		90		Orthorhombic Ag/α-MoO_3	Nanowires covered by Ag NPs	200-800	7-25

Journal of Materials Chemistry

Dynamic Article Links ►

Cite this: DOI: 10.1039/c0xx00000x

www.rsc.org/xxxxxx

Paper

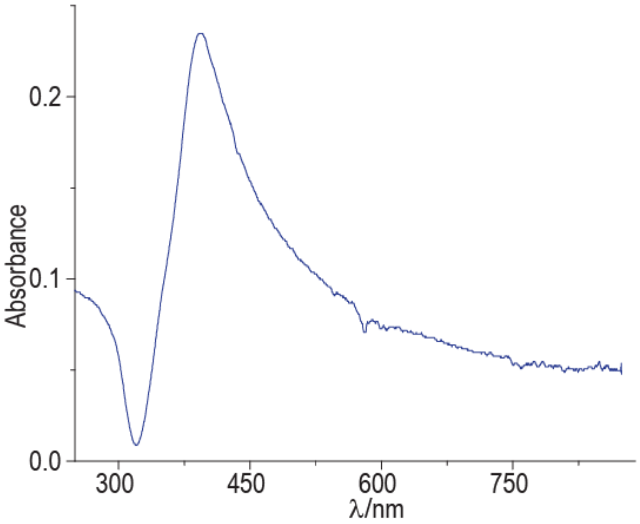

Fig. S3. UV-Vis spectrum of as synthesized Ag NPs

S2. As-synthesized Ag NPs absorption spectrum

The synthesized Ag NPs (**Fig. S3**) show a UV-Vis absorbance peak at λ ~400 nm which is in accordance with previous work.[S4] These kinds of Ag NPs have a size distribution between 9 and 15 nm.

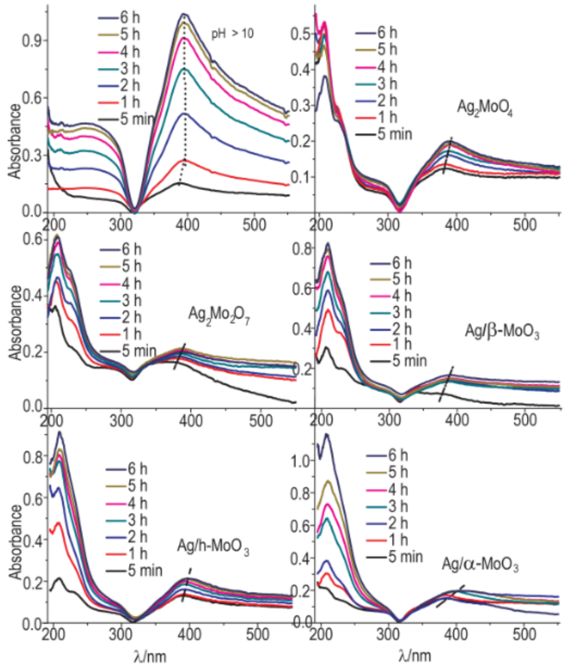

Fig. S4. Monitoring of $Ag_xMo_xO_{4x-1}$ transformation to Ag/Ag_2MoO_4 using UV-Vis spectroscopy.

S3. Conversion of $Ag_xMo_xO_{4x-1}$ ($Ag/\alpha\text{-}MoO_3$, $Ag/\beta\text{-}MoO_3$, $Ag/h\text{-}MoO_3$ and Ag_2MoO_7) binaries to Ag/Ag_2MoO_4

The transformation process of the mixture $Ag:Ag_xMo_xO_{4x-1}$ (x = 1, 2) in 97:3 %wt ratio was explored to determine the composition of the nanomaterials of SERS substrate ($Si@Ag/Ag_xMo_yO_z$). UV-Vis and Raman spectroscopy was used accordingly. **Fig. S4** displays the spectra recorded at different times after mixing Ag NPs and $Ag_xMo_xO_{4x-1}$. As can be seen, narrowing of the band peak between 320 and 440 nm (overlapping peaks of Mo^{6+} at ~350 nm and Ag NPs at ~400 nm towards ~400 nm) is observed, along with an increase in peak intensity (~230 nm and ~400 nm) with time. The disappearance of the peak at ~350 nm (narrowing of broad peak in the range 320-440 nm towards ~ 400 nm) could be due to the disappearance of Mo^{6+} in an octahedral coordination while the increase in peak intensity at ~230 nm and ~400 nm may be due to the appearance of Mo^{6+} in tetrahedral coordination, and the growth of Ag NPs size respectively. Such tetrahedral coordination environment only exists in Ag_2MoO_4.[S5] Furthermore, the Raman spectra obtained after 6 h reaction time (**Fig. S5**) showed the same profile and all the peaks are assigned to Ag_2MoO_4, thus confirming the results of UV-Vis. Accordingly, it is evident that $Ag_xMo_xO_{4x-1}$ is transformed to Ag/Ag_2MoO_4, and the transformation process seems to follow the reaction equation (S1) below:[S6]

$$Ag_xMo_xO_{4x-1} + xAg + \frac{1}{2}O_2 \rightarrow xAg_2MoO_4 \qquad \text{(S1)}$$

Where $x = \{1, 2\}$.

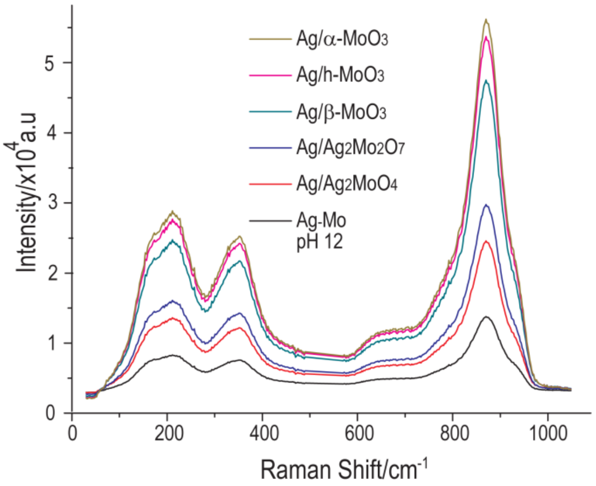

Fig. S5. Raman spectra of obtained product from the mixture of 97:3 %wt ratio of Ag NPs:$Ag_xMo_xO_{4x-1}$ after 6 h reaction time.

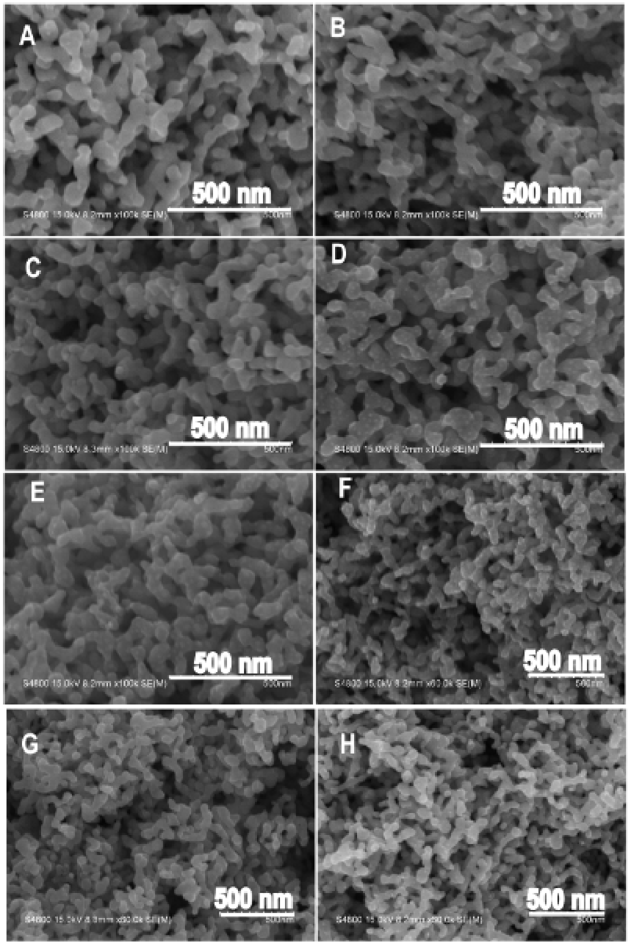

Fig. S6. SEM images of synthesized product by mixing Ag NPs and (A) Ag/α-MoO_3, (B) Ag/h-MoO_3, (C) Ag/β-Ag/MoO_3, (D) Ag/Ag_2MoO_7, (E) Ag_2MoO_4 and (F) Ag/Mo nanoclusters, (G) Ag/α-MoO_3 and (H) Ag NPs coated onto Si (Si@Ag/$Ag_xMo_yO_z$). (A-F) obtained using glucose as catalyst and (G) using cysteamine as catalyst.

S4. Comparison of SERS activity of Si@Ag/Ag_2MoO_4 fabricated using different $Ag_xMo_yO_z$

Different Si@Ag/Ag_2MoO_4 substrates were fabricated using 80 mL of Ag:Ag_xMoyO_z mixture. The fabrication procedure is described in **Experimental Section 2.4**. **Fig. S6** shows the SEM images of the obtained substrates. These substrates displayed have similar appearance. The deposited nanomaterials are constituted of Ag NPs with ~12 nm as diameter covering nanorods with ~40 nm and of 70-137 nm as width and length respectively. Besides, the fabricated substrates were studied (**Fig. S7**) applying 50 mL of 10^{-7} M R6G on the Si@Ag/$Ag_xMo_yO_z$ substrate and and driying the assembly at a steady temperature of 65 ^{o}C for ~1 h for SERS measurement. All substrates fabricated using Ag/$Ag_xMo_yO_z$ show the same profile. No shift in peak position was observed. However, a relative enhancement of Si@Ag/$Ag_xMo_yO_z$ compared to that fabricated using Ag NPs (Si@Ag), was obtained (**Fig. S6**B) with special mention for that obtained with Si@Ag/Ag_2MoO_4. The similar behavior for all Si@Ag/$Ag_xMo_yO_z$ substrates could be due to the fact that they have a similar structure (**Fig. S6**) and the final substrate is the same Si@Ag/Ag_2MoO_4. The enhancement of Si@Ag/Ag_2MoO_4 compared to Si@Ag could be due to the difference between the Plasmon wavelengths of the two nanomaterials. According to the UV-Vis absorption band (**Fig. S3** and **Fig. S4**), the plasmon wavelength of Ag is slightly higher than 400 nm while for Ag/Ag_2MoO_4 is around 390 nm. Meanwhile, the λ/2 of the Laser beam wavelength is 785/2 = 392.5 nm which is very close to the Plasmon wavelength of Ag/Ag_2MoO_4 than that of Ag used here. Si@Ag/Ag_2MoO_4 would therefore exhibit better enhancement than a simple Si@Ag.^{S7}

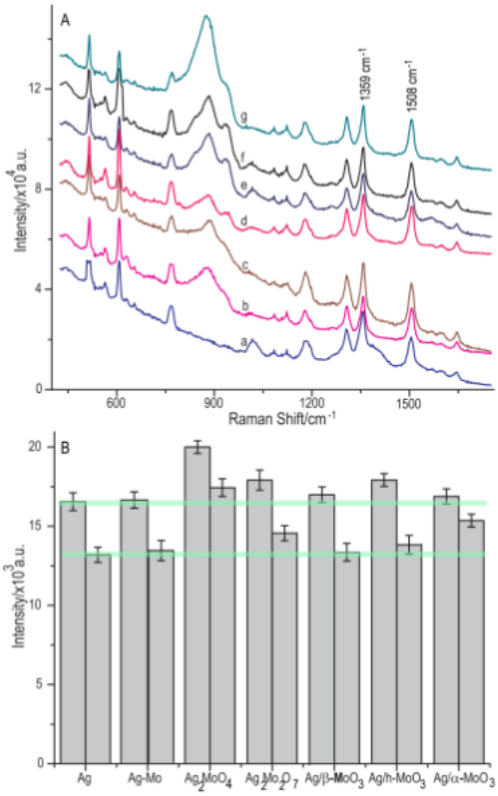

Fig. S7. (A) SERS spectra of 10^{-7} M R6G acquired from substrate based on (a) Ag NPs, (b) Ag-Mo, (c) Ag/Ag_2MoO_4, (d) Ag/$Ag_2Mo_2O_7$, (e) Ag/β-MoO_3, (f) Ag/h-MoO_3 and (g) Ag/α-MoO_3, and (B) SERS intensity of R6G peak centered at 1359 and 1508 cm^{-1}. Each data point represents the average value from three SERS spectra recorded from different substrates. Error bars show the standard deviations.

S5. Ability of retention of Si@Ag_2MoO_4

The capacity of retention of the analyte dropped on Si@Ag/Ag_4MoO_4 was studied by collecting at different weeks, the spectrum of 5×10^{-8} M R6G adsorbed on the Si@Ag/Ag_4MoO_4 substrate (**Fig. S8**). The spectra of the analyte obtained at different weeks were similar to that obtained freshly, neither a shift in major R6G Raman peaks nor significant changes in Raman intensity occurred. The intensities of R6G remained almost constant over the studied period with slight deviation not exceeding 3.1%, illustrating the ability of Si@Ag/Ag_4MoO_4 to be used for subsequent measurement over several weeks. This result also indicates that no particular condition is required to carry the sample dropped on the substrate for further long term measurement.

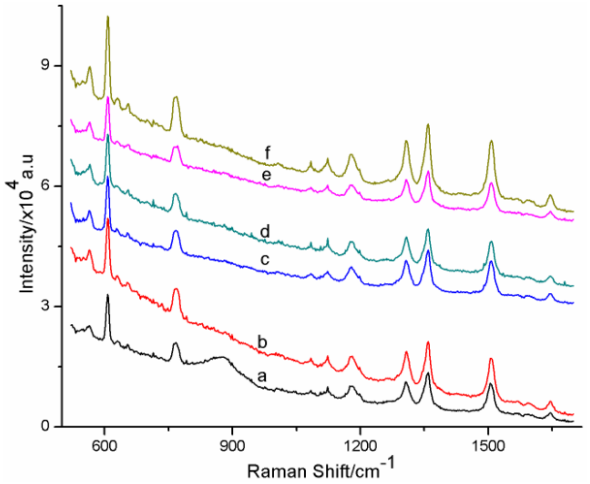

Fig. S8. Raman spectra collected from Si@Ag/Ag4MoO4 substrate stored with 10-7 M R6G at different weeks: (a) 0, (b) 1, (c) 2, (d) 3, (e) 4 and (f) 5 weeks.

However, it can be noticed that the peak at ~870 cm^{-1} disappeared after one week of storage of the substrate. This disappearance might suggest that Ag_2MoO_4 underwent relative deterioration. As Ag/Ag_2MoO_4 is known to be a good catalyst and as the SERS spectra are not really deteriorated, it can be assumed that Ag_2MoO_4 undergoes reduction and thus producing Ag and Mo and involving R6G degradation.[S8,S9] These new Ag NPs might maintain the SERS enhancement.

S6. Quantification of Si@Ag/Ag_4MoO_4

For a quantitative analysis, the SERS spectra of solution with different concentrations of R6G ranging from 1×10^{-14} to 3×10^{-12} M were measured. The SERS spectra of R6G adsorbed on the Si@Ag/Ag_2MoO_4 substrate, and the intensity profile of the peaks at 610, 1359 and 1508 cm^{-1} (assigned to the aromatic C–C ring in plane bend and stretching modes[S10]) as a function of the concentration of R6G are shown in **Fig. S9**A and **Fig. S9**B respectively. Increase in peak intensity as function of concentration was observed. It was found that each peak intensity was linearly proportional to the logarithmic concentration of R6G within the range of $1\sim300\times10^{-14}$ M with regression equations I (a.u.) = 97051.4+6902.3Log(C/M), R^2 = 0.91; I (a.u.) = 64199.0+4520.1Log(C/M), R^2 = 0.96 and I (a.u.) = 54430.3+3803.2Log(C/M), R^2 = 0.97 for 610, 1359 and 1508 cm^{-1} respectively. The observed limit of detection for R6G is 1×10^{-14} M, suggesting that Si@Ag/Ag_2MoO_4 has a good sensitivity.

The SERS enhancement factor (EF) is one of crucial parameter to demonstrate the performance of the substrate. Herein, we estimate this parameter from the standard equation defined as:

$$EF = \frac{I_{SERS}\times N_{RS}}{I_{RS}\times N_{SERS}} \qquad (S1)$$

where I_{SERS} and I_{RS} correspond to the Raman intensity of diagnostic band of the R6G adsorbed on the Si@Ag/Ag_2MoO_4 substrate and the normal Raman respectively; N_{SERS} and N_{RS} are the mole number of R6G under SERS and normal Raman conditions respectively, taking into account that the experimental conditions, such as the laser wavelength, laser power, microscope objective lens, and measuring conditions on the substrate are identical in all cases. N_{SERS} and N_{RS} are calculated using the **Equation S2** assuming that the surface A of the substrate is equivalent at any position point. As a result, a high EF of $\sim5\times10^8$ could be obtained when using C_{SERS} of 10^{-11} M (I_{SERS} = 14.1 u.a.) and W_{RS} of 1.2 mg (I_{RS} = 440.5 u.a.). The reason for this SERS performance may be attributed to the hot spots or active sites which could coexist between two adjacent Ag/Ag_2MoO_4 in the nanomaterials film. In this case, R6G molecules adsorbed on these hot spots or active sites might produce strong enhancement.[S11]

$$\frac{N_{RS}}{N_{SERS}} = \frac{f_{sh}N_{RS}}{\frac{\pi r^2}{A}N_0} = \frac{0.25\times N_{RS}}{78.5\times10^{-6}N_0} = 133\times\frac{W_{RS}}{C_{SERS}} \qquad (S2)$$

Where r = 5 µm is beam radius, No = V×C_{SERS} the mole number of R6G dropped on the substrate (V = 50 mL, the volume dropped on the substrate), N_{RS} =W_{RS}/M (M = 479 g/mol is molar mass of R6G) and A = 1cm×1cm the surface of Si sublayer. The factor f_{sh} takes into account the shielding of exciting and scattering of light by the nanoparticles. Here, 0.25 has been taken as f_{sh} value.

The enhancement could be due to the main role that might play Ag_2MoO_4 in this substrate. It is well known that the presence of nanomaterials supporting Ag nanoparticles could result in a largest electric field near the sharpest surface, thus increasing the local surface plasmon resonance and producing an excellent enhancement.[S12,S13] More hot spots or active sites could coexist between two adjacent Ag/Ag_2MoO_4 nanostructures in the film. In this case, R6G molecules adsorbed on these hot spots or active sites might produce strong enhancement.[S14]

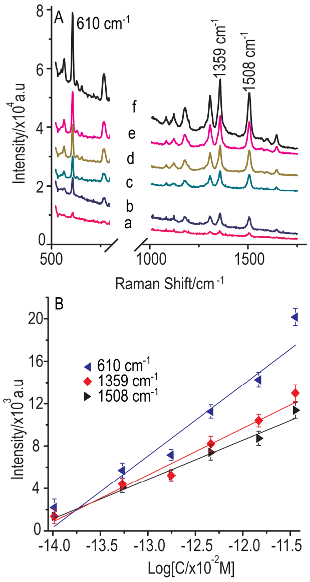

Fig. S9. (A) Raman spectra of R6G at different concentrations: (a) 1, (b) 5, (c) 15, (d) 50, (e) 125 and (f) 300×10^{-14} M, and (B) plots of intensity as a function of the logarithmic concentration of R6G at 610 cm^{-1}, 1359 cm^{-1} and 1508 cm^{-1}. Each data point represents the average value from three SERS spectra recorded from different substrates. Error bars show the standard deviations.

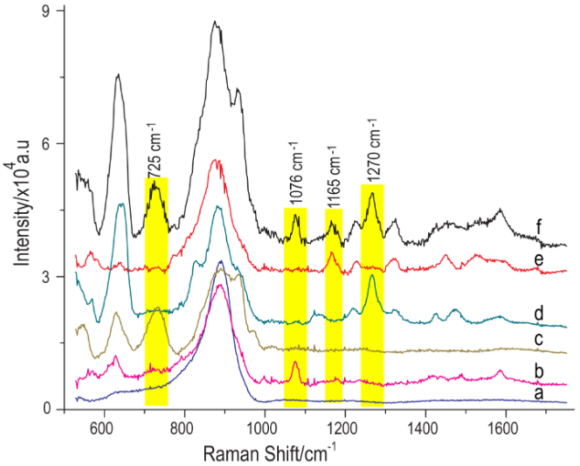

Fig. S10. Raman spectra of (a) Si@Ag/Ag_2MoO_4 substrate, (b) 5×10^{-6} M aniline, (c) 5×10^{-5} M ascorbic acid, (d) 1×10^{-7} M dopamine hydrochloride, (e) 5×10^{-9} M paraphenylenediamine and (f) their mixture.

S7. Determination of target molecule in complex matrices

Four target molecules (aniline, ascorbic acid, dopamine hydrochloride and para-phenylenediamine) were dropped on Si@Ag/Ag_2MoO_4 and dried . **Fig. S10** displays Raman spectra of individual analyte (**Fig. S10**b-e) and in their mixture (**Fig. S10**f). As highlighted in yellow, ring in plane deformation peak (1076 cm^{-1}) of aniline,[S15] OH out-of-plane deformation peak (725 cm^{-1}) of ascorbic acid,[S16] C-O-H symmetric in-plane bending vibrations of dopamine hydrochloride (1270 cm^{-1}),[S17] and C-H in plane bending vibration (1165 cm^{-1}) of para-phenylenediamine,[S18] could be used as specific peaks to detect the target molecule in the mixture.

Notes and references

[a] *Key Laboratory for Advanced Materials & Department of Chemistry. East China University of Science and Technology, 130 Meilong Road, Shanghai, 200237 P. R. CHINA, Tel./fax: +86-21- 64250032. E-mail: ytlong@ecust.edu.cn.*

[b] *Laboratoire de Chimie Physique. Université de Cocody. 22 BP 582 Abidjan 22, Abidjan, Côte d'Ivoire.*

S1 L. Cheng, Q. Shao, M. Shao, X. Wei, and Z. Wu, *J. Phys. Chem. C* **2009**, *113*, 1764.

S2 D. Stone, J. Liu, D.P. Singh, C. Muratore, A. A. Voevodin, S. Mishra, C. Rebholz, Q. Ge, and S. M. Aouadi, *Scripta Mater.* **2010**, *62*, 735.

S3 D. P. Singh, B. Sirota, S. Talpatra, P. Kohli, C. Rebholz, and S. M. Aouadi, *J Nanopart Res.* **2012**, *14*, 781.

S4 C.-N. Lok, C.-M. Ho, R. Chen, Q.-Y. He, W.-Y. Yu, H. Sun, P. K.-H. Tam, J.-F. Chiu, and C.-M. Che, *J. Proteome Res.* **2006**, *5*, 916.

S5 Y. V. Plyuto, I. V. Babich, I. V. Plyuto, A. D. V. Langeveld, and J. A. Moulijin, *Colloid Surface A* **1997**, *125*, 225.

S6 E. Wenda, *J. Therm. Anal.* **1998**, *53*, 861.

S7 E. Hutter and J.H. Fendler, *Adv. Mater.* **2004**, *16*, 1685-1706.

S8 M. Feng, M. Zhang, J.-M. Song, X.-G. Li and S.-H. Yu, *ACS Nano* **2011**, *5*, 6726-6735.

S9 J.C. Juarez and R. Morales, *Metall. and Mater. Trans. B* **2008**, *39*, 738-745.

S10 A. Weiss, and G Haran, *J. Phys. Chem.* B **2001**, *105*, 12348.

S11 E. K. Fodjo, S. Riaz, D.-W. Li, L.-L. Qu, N. P. Marius, T. Albert, and Y.-T. Long, *Anal. Methods* **2012**, *4*, 3785.

S12 J.-L. Yao, J. Tang, D.-Y. Wu, D.-M. Sun, K.-H. Xue, B. Ren, B.-W. Mao, and Z.-Q. Tian, *Surf. Sci.* **2002**, *514*, 108.

S13 L. M. Chen, L. B. Luo, Z. H. Chen, M. L. Zhang, J. A. Zapien, C. S. Lee and S. T. Lee, *J. Phys. Chem. C*, **2010**, *114*, 93.

S14 J. Hao, M. J. Han, Z. Xu, J. Li and X. Meng, *Nanoscale Res. Lett.*, **2011**, *6*, 263.

S15 M. Ilic, E. Koglin, A. Pohlmeier, H. D. Narres, and M. J. Schwuger, *Langmuir* **2000**, *16*, 8946.

S16 C. Y. Panicker, H. T. Varghese, and D. Philip, *Spectrochim. Acta A* **2006**, *65*, 802.

S17 S. Gunasekaran, R. Thilak Kumar, and S. Ponnusamy, *India J. Pure Ap. Phy.* **2007**, 45, 884.

S18 E. Akalin, and S. Akyuz, *J. Mol. Struct.* **2001**, *563-564*, 579.